

## CAV2009 – Paper No. 102

### A Multi-scale Study on the Bubble Dynamics of Cryogenic Cavitation

**Shin-ichi Tsuda**

Japan Aerospace Exploration Agency  
2-1-1 Sengen, Tsukuba-shi, Ibaraki, Japan

**Shintaro Takeuchi**

The University of Tokyo  
7-3-1 Hongo, Bunkyo-ku, Tokyo, Japan

**Yoichiro Matsumoto**

The University of Tokyo  
7-3-1 Hongo, Bunkyo-ku, Tokyo, Japan

**Mitsuo Koshi**

The University of Tokyo  
2-11-16 Yayoi, Bunkyo-ku, Tokyo,  
Japan

**Nobuhiro Yamanishi**

Japan Aerospace Exploration Agency  
2-1-1 Sengen, Tsukuba-shi, Ibaraki,  
Japan

#### ABSTRACT

This study aims to construct a multi-scale cavitation model for unsteady cryogenic cavitation CFD. Many elementary physical processes of bubbles (*i.e.*, nucleation, growth/shrink, evaporation/condensation, coalescence/fission, collapse, bubble-bubble interaction, bubble-turbulence interaction, and so on) emerge in cryogenic cavitation where some of the processes have not been understood well. In this paper, we mainly focused the molecular processes in homogeneous liquid-vapor nucleation with non-condensable gas solution by using Molecular Dynamics (MD) method. Bubble nucleation in liquid oxygen including helium, nitrogen, or argon was simulated. Molecular interaction was given by Lennard-Jones potential, and basically, each potential parameter was defined so that a saturation curve obtained by MD data was consistent with an experimental value. In the case that helium was impurity, a bubble nucleus was formed by density fluctuation at a lower concentration while a cluster constituted with helium molecules formed a bubble nucleus at a higher concentration, and the nucleation point becomes closer to the saturation point of pure oxygen when helium molecules form clusters. On the other hand, in the case that nitrogen or argon was the impurity, the above-mentioned clustering was not observed clearly at a concentration where helium made clusters, and these impurities have weaker action to make clusters and cavitation bubble nuclei compared with helium.

#### INTRODUCTION

Cryogenic fluids such as LNG (Liquified Natural Gas), liquid oxygen, liquid hydrogen, and liquid helium have been used in

many fields of engineering. At present these fluids are mainly applied in liquid rocket engines, power plants, superconductive coils, and so on. The demands for cryogenic fluids will greatly increase in the future. Since cryogenic fluids easily vaporize by heat entrance and/or cavitate in turbomachinery or pipes, the clarification of the liquid-vapor two-phase flows is very important in order to control these phenomena which result in the deterioration of performance or unstable oscillation. However, cavitating flows in cryogenic fluids have not been understood well compared with those of water at normal temperature because experimental approaches are not easy.

As one of unclear physical processes in cryogenic cavitation, we can refer to “nucleation”. It is known that vaporization of water at normal temperature occur at their saturation points in many cases, while cryogenic fluids do not often vaporize even if they exceed their saturation points. In such cases, a sudden rise of pressure with bubble formation or vapor explosion can occur in machines employing fluids. Therefore, the bubble formation mechanisms should be defined and the vapor points of cryogenic fluid must be estimated. Basic research on vaporization or the two-phase flow of cryogenic fluid has not been sufficiently conducted, and the mechanisms of these phenomena in such fluid are not fully understood.

Other than nucleation, as has been pointed out, so called “thermodynamic effect” is important in cryogenic cavitation. Although the characteristics have been investigated by some researchers [for example, 1-3] and the qualitative behavior becomes gradually clear, the quantitative detailed mechanisms are remained to be clarified. In addition, coalescence/fission, bubble-bubble interaction, and bubble-turbulence interaction, are also be understood furthermore although these processes are

important in all fluids other than cryogenic ones.

In this study, we are planning to construct a multi-scale/multi-process cavitation model which is necessary to realize an excellent cavitation Computational Fluid Dynamics (CFD) framework. Although cavitation CFD techniques have gradually been progressed by some groups [for example, 4-6], the quantitative accuracy is absolutely remained to be improved, particularly for cryogenic cavitation. To realize unsteady cavitation CFD, the modeling of cavitation is very important with the efforts to clarify unclear elementary processes mentioned above. In this paper, as the first step, we investigated the nucleation process in cryogenic cavitation from the molecular aspect.

## NOMENCLATURE

$k_B$	Boltzmann constant
$N$	number of molecules
$V$	volume of simulation cell
$T$	temperature
$t^*$	reduced time
$\rho^*$	reduced density
$p^*$	reduced pressure
$r$	distance between molecules
$m$	mass of each particle
$\sigma$	particle diameter of Lennard-Jones potential
$\varepsilon$	energetic depth of Lennard-Jones potential
SAT	saturation point
TLS	thermodynamic limit of superheating
KLS	kinetic limit of superheating

## FOR A MULTI-SCALE CAVITATION MODEL

In this chapter, our basic strategy for construction of a multi-scale cavitation model is simply described although many of the contents are undergoing. First, we investigate some microscopic effects of noncondensable gas on the homogeneous nucleation process of cavitation in cryogenic fluids (basically for liquid oxygen), using Molecular Dynamics (MD) method. The main purpose of this MD analysis is to study how the initial conditions for a macroscopic bubble should be given to the bubble dynamics analysis on the thermodynamic effects which will be conducted according to the method by Matsumoto and Takemura [7]. They investigated some phenomena inside of a bubble including thermal and transport processes. In this study, their method will be extended to the analysis on the thermodynamic effect in cryogenic fluids with an improvement of an equation of evaporation/condensation. We must accurately evaluate the mass flux of evaporation/condensation because this process is the source of the thermodynamic effect. Matsumoto and Takemura employed Shrage's form where evaporation/condensation was formulated based on Maxwell-Boltzmann distribution of gas molecules. Fujikawa's group has pointed out the non-equilibrium effect on evaporation/condensation is very important, and they recently have formulated some new boundary conditions for liquid/vapor interfaces [8]. Therefore, we will examine the new equation for evaporation/condensation with some improvements. Through these analyses, we will be able to extract some different mechanisms of growth/shrinkage of

cavitation bubbles from that in water, and obtained information is utilized to construct the new cavitation model. After the studies on the mentioned above, we will plan to extend the perceptions from single-bubble dynamics to multiple-bubbles. In this stage, we will employ an ensemble average method by Zhang and Prosperetti [9], and the main physical effects of the cavitation bubbles on the flow time scale are mainly extracted through time convolution. Through these processes, we will be able to evaluate important bubble physics which directly affects to the time scale of turbulent flow dynamics. (Other aspects such as turbulent modeling are also described in the appendix of "Work in Progress".) The quantitative physical values extracted by the time convolution will be integrated as a new multi-scale cavitation model that will provide the source term of mass, momentum, and energy of cryogenic fluids of interest.

## A MICROSCOPIC STUDY ON NUCLEATION

It should be mentioned that cavitation mostly originates from bubble nuclei, which consist of impurities, or at solid interfaces and has a great influence on bubble inception [10]. Therefore, these bubble nucleation mechanisms must be clarified to delineate bubble inception and the bubble formation points. Many researchers have studied these subjects from the viewpoint of classical theory and experiments [11], but most of these studies lack in the view of nanoscopic scale, which is one of the reasons why these phenomena have not been clarified. In the present research, therefore, computer simulations using the molecular dynamics method (MD) are applied to bubble nucleation in a cryogenic fluid which includes impurities. With this method, it is possible to research from the view of nanoscopic scale. Liquid oxygen including a non-condensable gas as impurities (*e.g.*, helium, nitrogen, or argon) was selected as the object of this simulation.

### Method

Using a microcanonical ensemble ( $NVE$ -constant) MD method, 10,976 molecules of liquid oxygen including helium, nitrogen, or argon were simulated. The computational domain was a cube imposed on the periodic boundary condition, and the volume was determined according to the density. All molecules were assumed to be monatomic to simplify the simulation. Therefore, these translational effects were estimated through this simulation, while those rotational effects as internal molecular freedom were not taken into consideration in the present study. Molecular interactions were simply given as the Lennard-Jones (12-6) potential as follows,

$$\varphi(r) = 4\varepsilon \left\{ \left( \frac{\sigma}{r} \right)^{12} - \left( \frac{\sigma}{r} \right)^6 \right\} \quad (1)$$

Assuming the Lorentz-Berthelot rules, all simulations were carried out after nondimensionalization of each physical value. Scaling parameters and their values are shown in Table 1. As a finite difference method of Newton's equations of motion, the leap-frog algorithm was chosen. To reduce the simulation time, cutoff distance  $r_c$  beyond which the interaction between each

[Type text]

Table 1. Scaling Parameters

Parameter	Unit	Value
Length	$\sigma$	$3.369 \times 10^{-10}$ m
Mass	$m$	$5.31 \times 10^{-26}$ kg
Time	$\sqrt{m\sigma^2/\epsilon}$	1.91 ps
Density	$m/\sigma^3$	1389 kg/m <sup>3</sup>
Pressure	$\epsilon/\sigma^3$	43.3 MPa

molecule can be neglected was employed.  $r_c=3.5\sigma$  was selected in this simulation, and the contribution of long range force on pressure and potential energy is also corrected if it was necessary.

First, an equilibrium state in which impurities were distributed uniformly at a constant concentration and temperature was produced. This equilibrium state was used as an initial condition, and the volume of the simulation cell and all molecular positions were expanded uniformly and instantaneously according to a final density to reduce the pressure and to simulate cavitation or degassing. All simulations were carried out at an average temperature of 90 K. In general, temperature is changed with expansion of the simulation cell when  $NVE$ -constant simulation is applied. Therefore, control of temperature should be carried out for a certain time to realize the objective temperature. In this simulation, temperature control was carried out by correcting each velocity of molecules by every 10 time-steps till  $t^* = 50$  (10,000 time-steps) after the simulation cell was expanded.

#### Definition of the Potential Parameters

First of all, Lennard-Jones potential parameters of each kind of molecule must be determined. In this study, the equation of state (EOS) obtained by Kataoka's method [12] was used to determine these parameters.

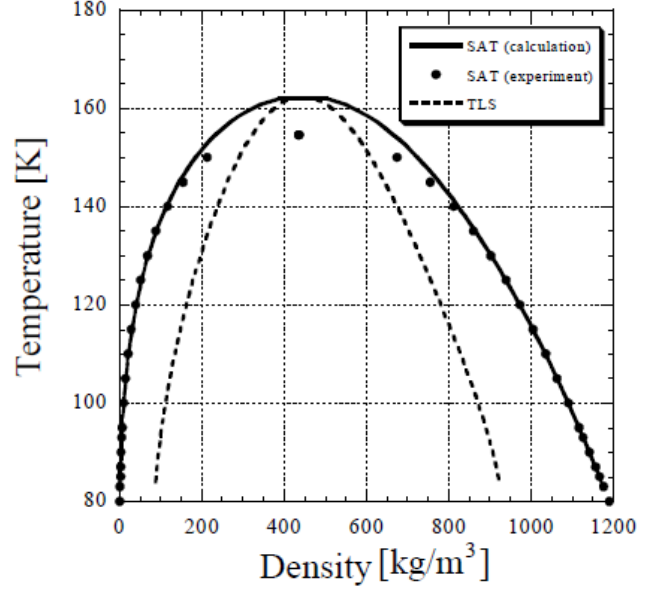
According to his method, EOS of the liquid-gas phase can be obtained by estimating excess Helmholtz energy  $A_e$  after subtracting the ideal gas term. This formula is

$$\frac{\beta A^e}{N} = \sum_{n=1}^5 \sum_{m=-1}^5 A_{nm} \left( \frac{\rho}{\rho_0} \right)^n \left( \frac{\beta}{\beta_0} \right)^m, \quad (2)$$

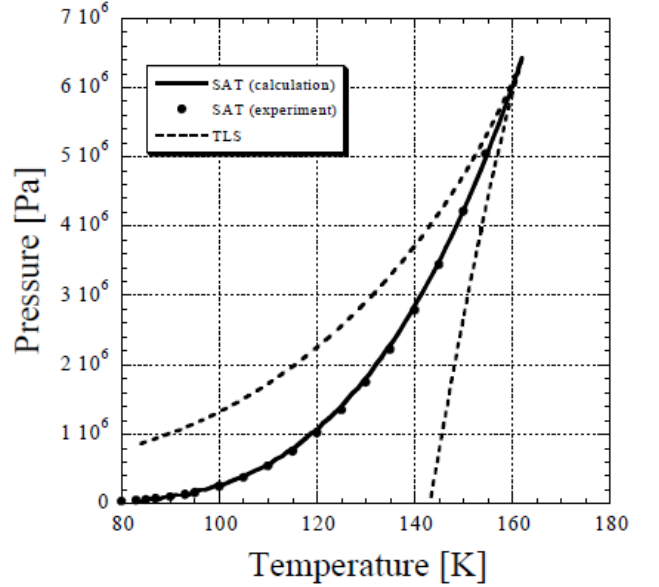
where  $\rho_0 = 1/\sigma^3$  and  $\beta_0 = 1/k_B T$  ( $\beta = 1/k_B T$ ). The relationship between internal energy  $E_p$ , pressure  $p$ , and  $A_e$  are expressed by the following forms,

$$E_p = \left( \frac{\partial (\beta A^e)}{\partial \beta} \right)_{\rho}, \quad (3)$$

and



(A)



(B)

Fig. 1. Saturation Line and Spionodal Line for Oxygen. (A) Density-Temperature Curve, (B) Temperature-Pressure Curve

$$\frac{\beta A^e}{N} = \int_0^p \frac{(\beta p / \rho_0 - 1)}{\rho} d\rho. \quad (4)$$

In this method, the coefficients of equation (4),  $A_{nm}$ , are defined by using MD data. Therefore, MD simulations were executed at various density-temperature points, and the values of  $E_p$  and  $p$  at the respective density-temperature points were obtained by taking the respective time averaged values of the

Table 2. Parameters of Each Molecule

Molecule	$m$ [ $\times 10^{-27}$ kg]	$\epsilon/k_B$ [K]	$\sigma$ [ $\times 10^{-10}$ m]
Oxygen	53.1	120.0	3.369
Helium <sup>[14]</sup>	6.65	6.030	2.630
Nitrogen	46.5	99.03	3.594
Argon	66.3	115.5	3.385

equilibrium state. Each MD simulation was executed by using 864 molecules. It was predicted that there might be density-temperature points of solid state among MD simulation points. Since EOS expresses the gas-liquid region, MD simulation points of the solid state should not be employed. Therefore, the points where the mean square displacement takes less than  $5\sigma$  was regarded as the solid state, and these points were rejected in this study. This was based on the fact that the mean square displacement of a solid is about  $1\sigma$ , while on the order of  $100\sigma$  in the liquid state at the present simulation time. It was also predicted that there might be density-temperature points of the state where liquid and gas phases would coexist among MD simulation points; they were also rejected. It has been reported that pressure and temperature greatly change if an initial liquid state changes to a two-phase state in such a molecular system [13]. Therefore, the MD simulation point where the difference of temperature between the simulated value and the initial one exceeds 0.05 of that initial one was regarded as a two-phase state, and these points were rejected when EOS was calculated. Using  $E_p$  and  $p$  obtained by MD simulations, the coefficients,  $A_{mn}$ , were defined by using the least-square method.

The procedure to define each potential parameter was as follows. First, initial potential parameters were given as the values which are obtained from the viscosity data of gas [14], and MD simulation was executed under those potential parameters. Next, EOS was calculated by using that MD data and the saturated liquid density and temperature under the atmospheric pressure ( $1.01 \times 10^5$  Pa) obtained by the EOS was compared with the experimental values. Each potential parameter was corrected so that the saturated density and temperature obtained by the EOS were consistent with the experimental values. The procedure of the MD simulation, the calculation of EOS, and the correspondence of each potential parameter was repeated till the error of that density is below 1 kg/m<sup>3</sup> and that of that temperature is below 0.5 K. As mentioned above, the final Lennard-Jones potential parameters of each kind of molecule are defined as shown in Table 2. Figure 1 shows the saturation line and spinodal line calculated by Kataoka's method. It is obvious that the calculated saturation line is consistent with that of the experiment except around the critical temperature.

In this research, each kind of potential parameters was defined so that the liquid expressed by the determined potential parameters can simulate the thermodynamic properties of each liquid, except helium. Therefore, in this study, each potential parameter was determined so that each saturation curve obtained by Kataoka's method corresponds to the experimental one. Since helium at  $T = 90$  K further exceeds the critical

temperature, it is worth nothing that the potential parameters for helium which are defined to express an experimental saturation curve accurately. In this study, the potential parameters of helium were selected so that the second-virial coefficient is consistent with the experimental value [14], because it is known that the potential parameters which are determined well express the thermodynamic properties in such a supercritical state where the molecular interaction is very weak. Each potential parameter is shown in Table 2.

## Results

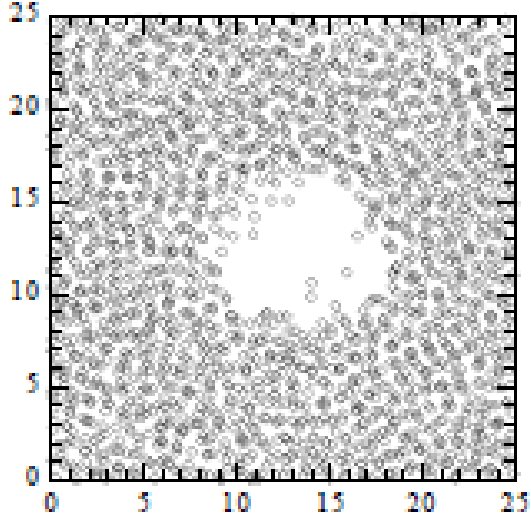
Bubble nucleation is caused by the density fluctuation or by the clustering of impurities. The following points should be mentioned about the bubble formation point. When the pressure of a liquid is lower than the saturation point (SAT) but higher than the thermodynamic limit of superheating (TLS), where liquid state is absolutely unstable, bubble formation is dependent on the amount of disturbance which is based on the density fluctuation or the clustering of impurities. In the present research, the Kinetic Limit of Superheat (KLS), which is the lowest density or pressure where a bubble is not formed, is predicted by using MD simulation. It should be pointed out that KLS depends on the simulation domain size [15] and that KLS moves closer to SAT as the size increases. Hence, KLS determined in the present study is not the macroscopic bubble formation point. Paying attention to the above-mentioned factor, MD simulations are carried out at some density points which belong to the area between SAT and TLS at  $T = 90$  K to determine the bubble nucleation mechanism and the variance of KLS.

### (Case1: Pure Oxygen)

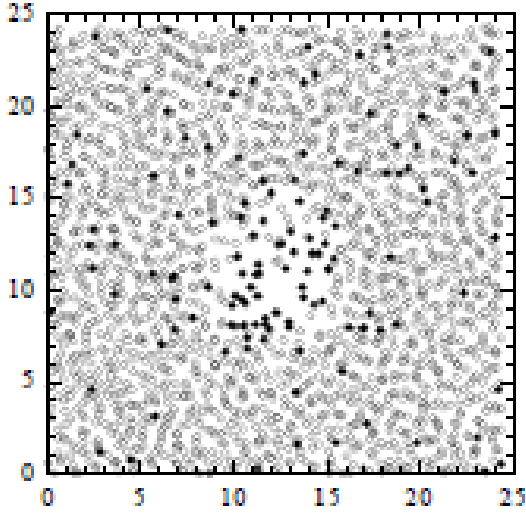
First of all, KLS of liquid oxygen was estimated for comparison with the bubble formation point of the cases in which impurities are included. The density of initial condition,  $\rho_{mi}^*$ , was set at 0.850 in every simulation, and each final reduced density of simulation points,  $\rho_{fin}^*$ , was basically decreased by 0.010. In the present simulations, a bubble was formed from a certain time when  $\rho_{fin}^* = 0.715$  or less. Hence, in our research, the density at KLS was determined as  $\rho_{fin}^* = 0.725$ , which was considered to be the lowest density where bubble formation is not observed. In Fig. 2 (A), a photograph that expresses one of the sections in which the simulation cell was divided into five areas is shown.

### (Case2: Helium)

MD simulations were executed at some density points in the case that helium molecules are impurities under the following two conditions;  $c = 0.01$  and  $c = 0.05$ . In the case of  $c = 0.01$ , a bubble was formed when  $\rho_{fin}^* = 0.725$  or less, and the bubble formation mechanism was similar to the case of pure oxygen. At least, clustering of impurities was not observed clearly when  $\rho_{fin}^*$  had been decreased by 0.010 till a bubble was formed, where clustering of impurities was analyzed as follows: a cluster was defined if two molecules are continuously connected for less than a distance of  $1.5\sigma_N$ , and the number of the molecules which belong to the largest cluster in the simulation cell,  $n_{clus}$ , at each time step was recorded. In this case,  $n_{clus}$  always took a low value which is no more than 10. Therefore, bubble nucleation was considered to be caused by density fluctuation at  $c = 0.01$ . As shown in Table 3, both of the



(A)



(B)

Fig.2 Snapshots of a Formed Bubble Nucleus. (A) Pure Oxygen, (B) Oxygen with Helium ( $c=0.05$ ). (white circle; oxygen, black circle; helium)

density and the pressure at KLS showed larger values than that of pure oxygen, and bubble formation occurred at the point where it did not occur in the unary system. This means that helium molecules exert some influence on bubble nucleation. Considering that the bubble nucleation in this case was not caused by clustering of impurities, it is supposed that the amount of the density fluctuation is larger than that in the case of pure oxygen. In the case of  $c=0.05$ , clustering of helium molecules was observed at  $\rho^* = 0.760$  when  $\rho^*_{fin}$  was decreased by 0.010. The photograph showing each molecular position at  $t^*=300$  are presented in Fig. 2 (B). At this condition, no obvious void like Fig. 2 (A) was observed. As mentioned above, it is

Table 3 KLS of Each Case ( $T=90K$ )

Impurity	Concentration [-]	Density [-]	Pressure [-]
None	0.00	0.725	-0.761
Helium	0.01	0.735	-0.708
Helium	0.05	0.760	-0.531
Nitrogen	0.05	0.710	-0.735
Argon	0.05	0.725	-0.759

known that whether a bubble is formed or not depends on the amount of disturbance which is based on density fluctuation or clustering of impurities when the liquid is in a metastable state. Therefore, if this state emerges on a considerably larger scale, it is probable that clustering of impurities causes a bubble of oxygen due to the existence of a larger disturbance than is necessary for bubble formation. If the computational domain is larger, it is probable that the concentration at which clustering occurs becomes low, but the tendency of bubble formation due to density fluctuation when the concentration is low and formation of clusters of helium molecules when the concentration is high, is not changed.

(Case3: Nitrogen or Argon)

MD simulations were executed in the case of nitrogen or argon at the concentration of 0.05. The density and pressure at KLS in each case, which were defined by the present simulations, are also shown in Table 3. In these cases, the molecules of nitrogen or argon did not form a distinct cluster, and a bubble was formed by density fluctuation. This was confirmed by the result that  $n_{clus}$  at each simulation time had a low value less than 2 or 3 throughout the simulation. Therefore, the bubble nucleation mechanism in these cases is considered to be density fluctuation. When nitrogen is dissolved in liquid oxygen, the density at KLS is lower, but the pressure at this point is higher than those of pure oxygen, while in the case in which argon is included, these values are almost as same as those for pure liquid oxygen. Considering that clustering of impurities is not evident in either case, these differences of KLS can be explained by the amount of density fluctuation. Namely, the density fluctuation in the case of nitrogen is smaller than in the pure case. The reason for this is considered to be that the diameter of nitrogen is larger than that of oxygen. (Detailed investigation of this point, however, is necessary.) While in the case of argon, these potential parameters are very close to those of oxygen. Therefore, it is considered that the bubble formation mechanism and the bubble formation point are almost the same as those of unary liquid oxygen. If the concentration is increased or the computational domain becomes larger, clustering may occur as is the case with helium. However, that helium has a stronger action to make a cluster than nitrogen or argon is not changed. Therefore, it is considered that a bubble is still formed by density fluctuation even in the range of concentration where is already formed by clustering of helium molecules.

## CONCLUSION

In this paper, as a previous step to construct a new multi-

scale cryogenic cavitation model, Molecular Dynamics (MD) simulations of liquid oxygen including helium, nitrogen, or argon were executed to understand the bubble nucleation mechanism and the difference of Kinetic Limit of Stability (KLS) from the kinetic point of view at a microscopic scale. When helium is dissolved in liquid oxygen, it was verified that bubble nucleation is caused by density fluctuation at a lower concentration while it is caused by clustering of helium at a higher concentration. Moreover, in the case in which helium makes a cluster, the bubble formation point moves closer to saturation point of pure oxygen compared with the case of nitrogen or argon. When nitrogen or argon is included as an impurity, it was considered that there is a concentration range where helium has already formed clusters, and a bubble is formed by clustering while nitrogen or argon does still not form clusters and is formed by density fluctuation. Since nitrogen or argon is included at a much higher concentration, however, it is probable that these impurities form clusters and that a bubble is formed by clustering. Further investigation is necessary to clarify this point, and we are planning to propose a kinetic nucleation model which will be installed to a new multi-scale cryogenic cavitation model.

## APPENDIX

### Work in Progress

As is described, this study finally aims for development of a total numerical analysis tool for predicting unsteady cryogenic cavitating flows. For this purpose, the authors have the following components in mind with the relatively higher priority to be integrated with a new cavitation model;

- (1) turbulent model of bubbly flow,
- (2) viscous dissipation at the inducer walls.

For the first item, we have already derived a liquid flow model at a high void fraction condition under free-slip assumption. It would help development of a turbulent model. The validity and applicability of the model will be assessed in a bubbly flow with the methods that offer very sharp interface between gas and liquid; *e.g.*, front-tracking method [16, 17]. Also, the model will be tested by incorporating into a practical cavitation flow solver. The model still needs to be focused on the incorporation of the effect of compressibility of the bubbles, but it would be at the next stage.

The effect of the second item would specifically important in cryogenic fluids. The authors are ready to launch a one-fluid model that covers gas, liquid and solid wall including the effect of heat source at the solid walls. The model will be coupled with the momentum equation for the three phases by an immersed-boundary model by the present authors [18, 19]. The method has enabled simulations of flow patterns in very complex configurations of relative motions between bubbles and solid particles of comparable sizes, including the flow pattern around the gas-liquid and solid-liquid interfaces.

The authors believe that construction of a new multi-scale/multi-physics cavitation model which would yield an invaluable practical analysis tool of cryogenic cavitation, will be enable by combing these proposed treatments for turbulence and multi-body problem.

## REFERENCES

- [1] A. J. Stepanoff, "Cavitation Properties of Liquids", ASME Journal of Engineering and Power **86**, pp.195-200, (1964).
- [2] J. P. Franc et al., "An Experimental Investigation of Thermal Effects in a Cavitating Inducer", ASME Journal of Fluids Engineering **126**, pp.716-723, (2004).
- [3] Y. Yoshida et al., "Thermodynamic Effect on a Cavitating Inducer in Liquid Nitrogen", ASME J. Fluid Eng. **129**, pp.273-278, (2007).
- [4] Schnerr, G. H., "Modeling of Unsteady Cavitating Flows: Status and Future Development", Proc. of 6th ISAIF, pp. K1-K21., (2003).
- [5] Y. Iga et al., "Numerical Analysis of Sheet Cavitation Breakoff Phenomenon on a Cascade Hydrofoil", ASME Journal of Fluids Engineering **125**, pp.643-651, (2003).
- [6] H. Hosangadi and V. Ahuja, "A Numerical Study of Cavitation in Cryogenic Fluids Part II; New Unsteady Model for Dense Cloud Cavitation.", Proc. of 6th International Symposium on Cavitation (CD-ROM), (2006).
- [7] F. Takemura and Y. Matsutomo, "Influence of Internal Phenomena on Gas Bubble Motion (Effects of Transport Phenomena and Mist Formation inside Bubble in the Expanding Phase)", JSME International Journal, Series (B) **37**, pp.736-745, (1994).
- [8] T. Ishiyama et al., "Kinetic Boundary Condition at a Vapor-Liquid Interface", Phys. Rev. Lett. **95**, 084504, (2005).
- [9] D. Z. Zhang and A. Prosperetti. "Ensemble phase averaged equations for bubbly flows", Phys. Fluids **6**, pp.2956-2970, (1994).
- [10] Debenedetti, P.G., "Metastable Liquids -Concepts and Principle-", Princeton University Press, (1996).
- [11] M. Blander and J. L. Katz, "Bubble Nucleation in Liquids", AIChE Journal **21**, pp.833-847, (1975).
- [12] Kataoka, Y., "Studies of liquid water by computer simulations. V. Equation of state of fluid water with Carravetta-Clementi potential", Journal of Chemical Physics **87**, 589-598, (1987).
- [13] Kinjo, T. and Matsumoto, M., "Cavitation processes and negative pressure", Fluid Phase Equilibria **144**, pp.343-350,(1998).
- [14] J. O. Hirschfelder, et al., "MOLECULAR THEORY of GASES and LIQUIDS", John Wiley & Sons, Inc.,1954.
- [15] S. Park et al., "Cavitation and Bubble Nucleation Using Molecular Dynamics Simulation", Microscale Thermophysical Engineering **4**, pp.161-175, (2000).
- [16] S. O. Unverdi and G. Tryggvason, "A Front-Tracking Method for Viscous, Incompressible, Multi-fluid Flows", J. Comput. Phys. **100**, pp.25-37, (1992).
- [17] G. Tryggvason et al., "A Front Tracking Method for the Computations of Multiphase Flow", J. Comput. Phys. **169**, pp.708-759, (2001).
- [18] R. Iwata et al., "Analysis of Collective Behavior of Bubbles and Particles in Liquid Flows by a Coupled Immersed-Boundary and Volume-of-Fluid Method", Academy Colloquium Immersed Boundary Methods:

[Type text]

Current Status and Future Research Directions,  
Amsterdam, The Netherlands, 15-17 June (2009).

- [19] R. Iwata et al., "Direct Numerical Simulation of Three-phase Flows using Immersed Boundary Method Coupled with Volume of Fluid Method", *Int. J. Multiphase Flow*, submitted.